Chemosphere 308 (2022) 136530

Contents lists available at ScienceDirect

Chemosphere

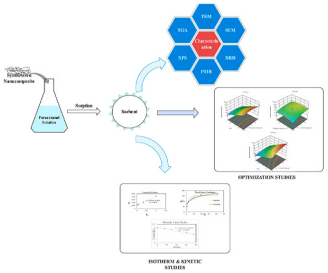
journal homepage: www.elsevier.com/locate/chemosphere

Synthesis of metal-based functional nanocomposite material and its application for the elimination of paracetamol from synthetic wastewater

HIGHLIGHTS

- A novel TiO_2/Fe_2O_3/Chitosan Nanocomposite was synthesized.
- Synthesized nanocomposite was characterized by SEM, TEM, XPS, TGA, FTIR, XRD.
- Maximum sorption of paracetamol at optimized conditions was 90.26%.
- Langmuir Isotherm fits the sorption data with $R^2 > 0.9481$
- Sorption follows Pseudo First Order reaction with R^2 value of more than 0.9481

GRAPHICAL ABSTRACT



ARTICLE INFO

Handling Editor: Fateme Karimi

Keywords:
Pharmaceuticals
Nanocomposite
Contaminants
Moringa olifera
Isotherm
Kinetics

ABSTRACT

Non-steroidal anti-inflammatory medicines (NSAIDs) like paracetamol and other substances released into the water system pose serious environmental issues. The current work examines the synthesis of a nanocomposite combined with *Moringa olifera* aqueous leaf extract as a reducing and stabilizing agent for the green synthesis of nanocomposites. Fourier Transform Infrared Spectroscopy (FTIR), X-ray Diffraction (XRD), Thermogravimetric analysis (TGA), Scanning Electron Microscope (SEM), Transmission Electron Microscope (TEM) were used to investigate metal based functional nanocomposites. The absorption band centered at a wavelength of 243 nm, which corresponds to the surface plasmon resonances of the produced nanocomposite, is confirmed in UV–vis spectra. The distinctive band at this particular wavelength is attributed to a particular group of nanocomposites based on the result from the Fourier transform infrared spectroscopy spectra. The spherical with irregularly shaped aggregates was confirmed by transmission electron microscopy, and the average size of nanoparticles was found to be 1 nm. For the elimination of pharmaceutical contaminants such as paracetamol from aqueous solutions, the adsorptive characteristics of nanocomposites were examined. Temperature, pH, adsorbent dosage, and agitation speed were investigated as adsorption parameters using Box-Behnken Design (BBD). The best removal outcomes were found under the following circumstances: temperature at 303.15 K, pH = 7.5, 0.05 g of nanocomposites at 200 rpm. Based on the adsorption study, the kinetics was found to be pseudo first order ($R^2 > 0.9481$) which was validated and fitted by Langmuir isotherm ($R^2 > 0.9973$). The adsorption study confirms that it was adsorbed onto the synthesized nanocomposite and found to be present on the homogeneous surface.

* Corresponding author.
E-mail address: rajamehala@gmail.com (M. Rajamehala).

https://doi.org/10.1016/j.chemosphere.2022.136530
Received 30 June 2022; Received in revised form 10 September 2022; Accepted 15 September 2022
Available online 20 September 2022
0045-6535/© 2022 Elsevier Ltd. All rights reserved.

1. Introduction

With the rapid development in technology, day by day the lands were utilized by different industries for various purposes in different sectors for the welfare of human being. Due to the enormous growth of industries, wastes are generated in plenteous amount and it is being released into the water stream and land. These wastes pose a serious threat to the human beings and environment at an alarming rate in generation of pollutants, (Mane et al., 2018). The arrival of modern technologies and due to change in food habitats lead to several kinds of incurable diseases in human being. New medicines were produced continuously by pharmaceutical industries (Chandrashekar Kollarahithlu and Balakrishnan, 2021). These pharmaceutical industries uses both organic and inorganic raw materials for their production and the waste discharged by them turn toxic to biological life (Ferrari et al., 2003). When the drugs are consumed by humans for therapeutic purpose, it undergoes different metabolic reactions inside the human body and excreted and it is released into the water and affects the environment. The pharmaceutical wastes that discharged in to the water bodies cause genotoxicity, acute toxicity, carcinogenicity and also cause some mutagenic effects. This pharmaceutical pollutant is an emerging one among others (Żur et al., 2018). Commonly detected drug components in pharmaceutical waste discharges are paracetamol, anti-inflammatory, anti-depressants, aspirin, contraceptives and anti-epileptics. Among these paracetamol-based medication wastes were detected as larger amount, which is because it has been used as first-aid medicine for common body pain and fever by people all over the world (Mane et al., 2018). Some of the research work carried out by researchers have proven the occurrence of drugs in drinking water (211 nhL^{-1} concentration level) (Hinson et al., 2004; Rabiet et al., 2006; Żur et al., 2018; Liu et al., 2021a,b; Tayyab et al., 2022).

Wide varieties of techniques are available for the removal of pharmaceutical pollutants from water which includes biological, physical and chemical methods. The main disadvantages associated with them is the generation of enormous amount of sludge and finding remedy for their disposal. Recent years, a method that has gained interest among the researchers in pharma pollutant removal is advanced oxidation process method (AOP). Yet the use of large amount of chemicals and high energy consumption made it difficult for the process to succeed in the industrial application. Therefore, there is no efficient method were developed for removing these kinds of micro pollutants (Candido et al., 2017). Very low volume of pharmaceutical pollutants like paracetamol, antibiotic trimethoprim, etc., were removed with help of entire wastewater treatment processes. Therefore, several approaches based on bio components such as nanocomposites were invented by scientific communities to overcome this scarcity (Yang et al., 2017).

The removal of pharma pollutants with help of nanocomposites were performed based upon the adsorption theory. Here the presence of pharma pollutants in environmental resources was adsorbed by nanocomposites containing specific charged functional groups on its 3D structure. Therefore, in this study we have developed the nanocomposite with help of TiO_2/Fe^{3+}/Chitosan for removal of paracetamol pollutants from pharmaceutical waste. The scientific reports from (Pişkin et al., 2013) shows the positive results about the attention of TiO_2 nanoparticles on removal of organic pollutants. Usually, the TiO_2 have optical photo catalytic and dielectric features, so that it gives more attention in organic pollutant removal strategy. At present TiO_2 with different formulations has been utilized in many applications related to pollution control (Pişkin et al., 2013). Chitosan gives crucial support to the adsorption of drug molecules on its structure and can be considered as efficient polymeric material for removal of pharmaceutical pollutants from environmental sources (Blackburn, 2004; Ciesielski et al., 2003; Crini, 2006). Nanocomposite based on TiO_2, Fe^{3+} and biopolymer (chitosan) act as good base material for adsorptive removal of organic pollutants like paracetamol from pharmaceutical waste. The presence of those components in nanocomposites causes the stable affinity for paracetamol pollutants.

Management of these pollutants by the researchers around the globe is still a hurdle and has attracted them to find a novel remedy. The prevailing study aims in development of a simple method for the pollutant's removal. Several new strategies are proposed to improve the performance of sorption and here TiO_2/Fe_2O_3/Chitosan nanocomposite is used and various parameters have been optimized in order to obtain the maximum removal.

2. Materials and methods

Chemicals of analytical grade were used. Titanium isopropoxide, Ferric chloride and Chitosan were procured from Merk Ltd, India. 0.1 Molarity of HCl and NaOH were used to alter the pH of the solution used for the study. UV Spectrophotometer (Shimadzu UV-1700 spectrophotometer) is used for estimating the concentration of the samples. Sonicator (Bandelin Sonoplus HD-2070) is used for homogenizing the composite.

2.1. Preparation of Moringa olifera leaf extract

Moringa olifera leaves were collected from Tiruchengode, Tamilnadu. Leaves were washed once in tap water and twice in double distilled water to remove impurities. They were then dried in sunlight for 24 h

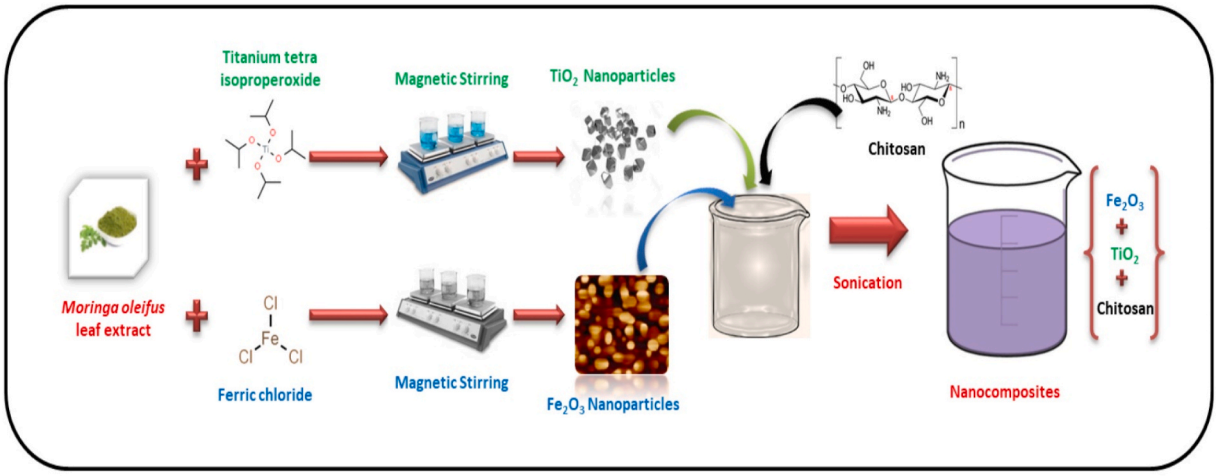
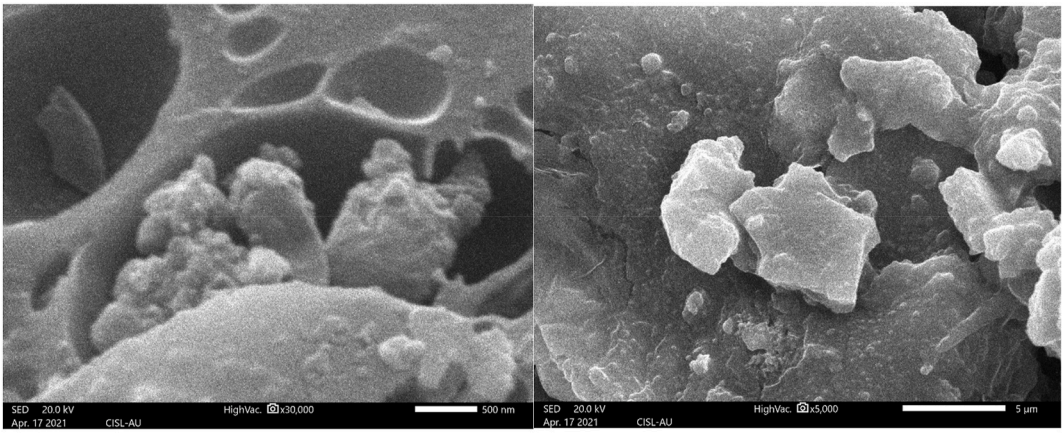
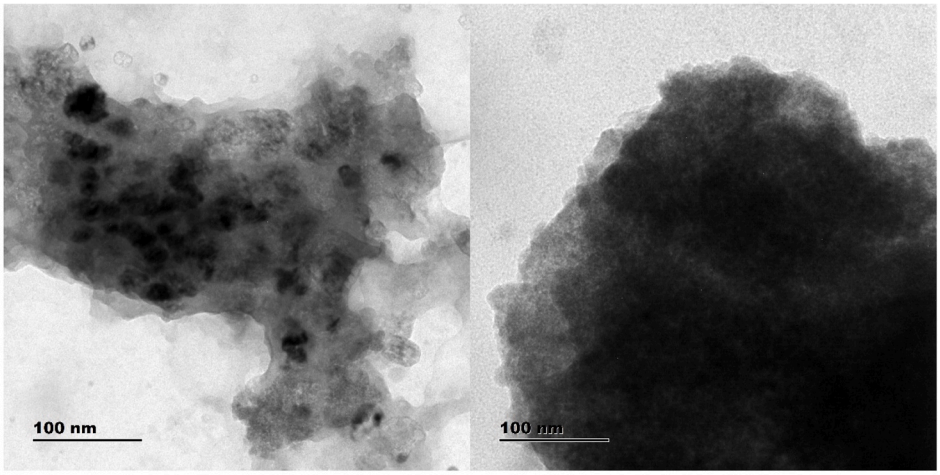


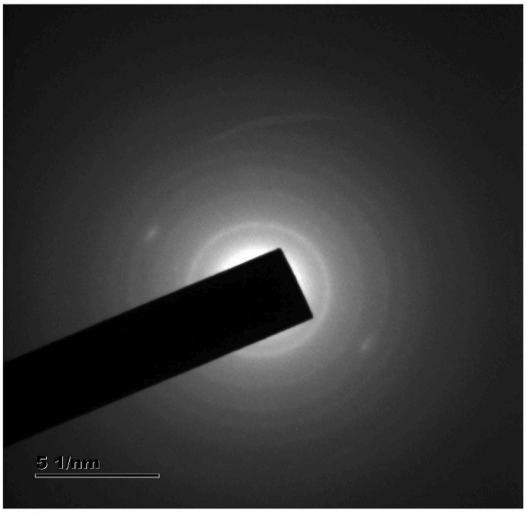
Fig. 1. Schematic diagram for the sorption of paracetamol from aqueous solution.



a SEM images of TiO_2-Fe_2O_3-chitosan sample

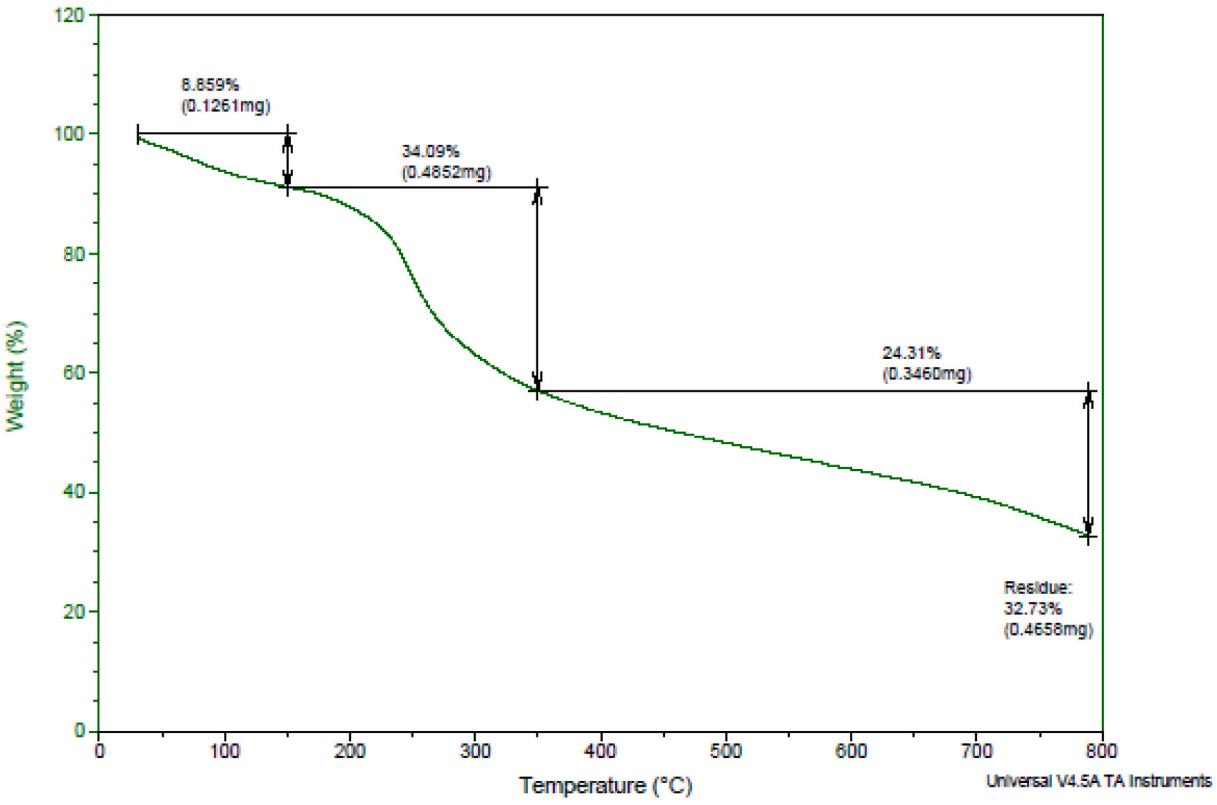


b HRTEM images of TiO_2-Fe_2O_3-chitosan sample

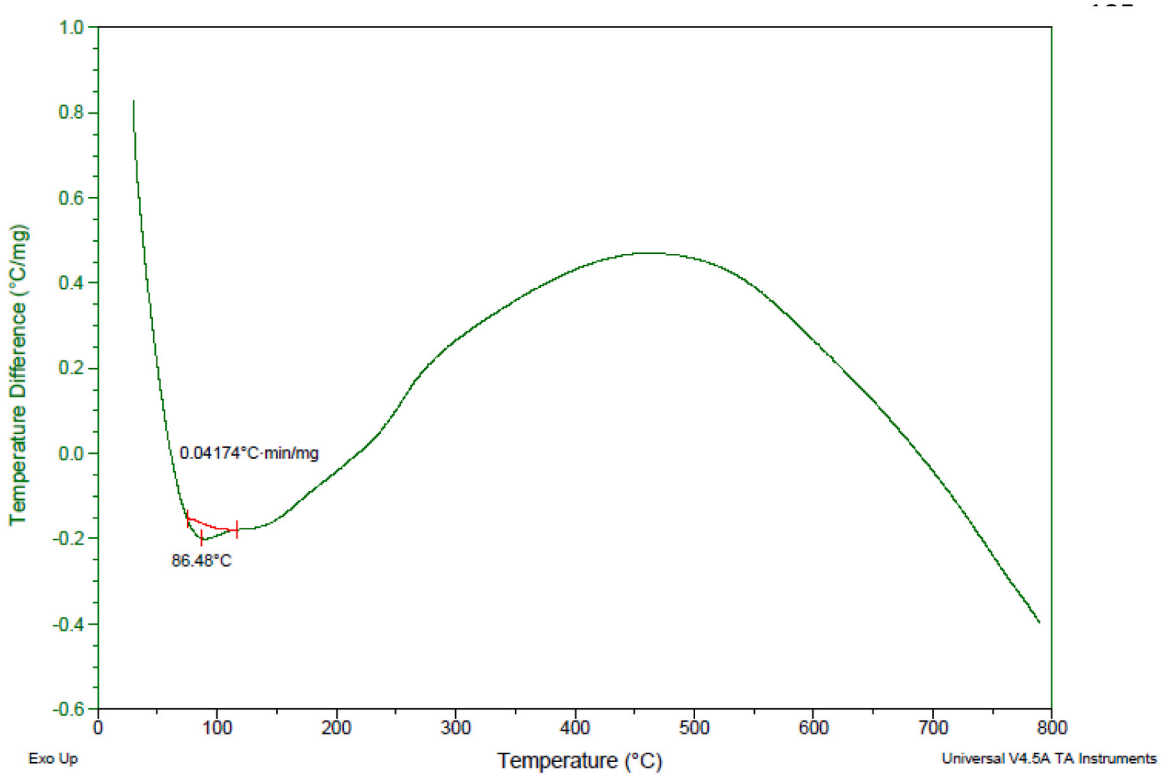


c HRTEM – SAED pattern of TiO_2-Fe_2O_3-chitosan sample

Fig. 2. a SEM images of TiO_2-Fe_2O_3-chitosan sample
b HRTEM images of TiO_2-Fe_2O_3-chitosan sample
c HRTEM – SAED pattern of TiO_2-Fe_2O_3-chitosan sample.



a. TGA analysis of synthesized metal based nanocomposite



b. TGA analysis of synthesized metal based nanocomposite

Fig. 3. a. TGA analysis of synthesized metal based nanocomposite
b. TGA analysis of synthesized metal based nanocomposite.

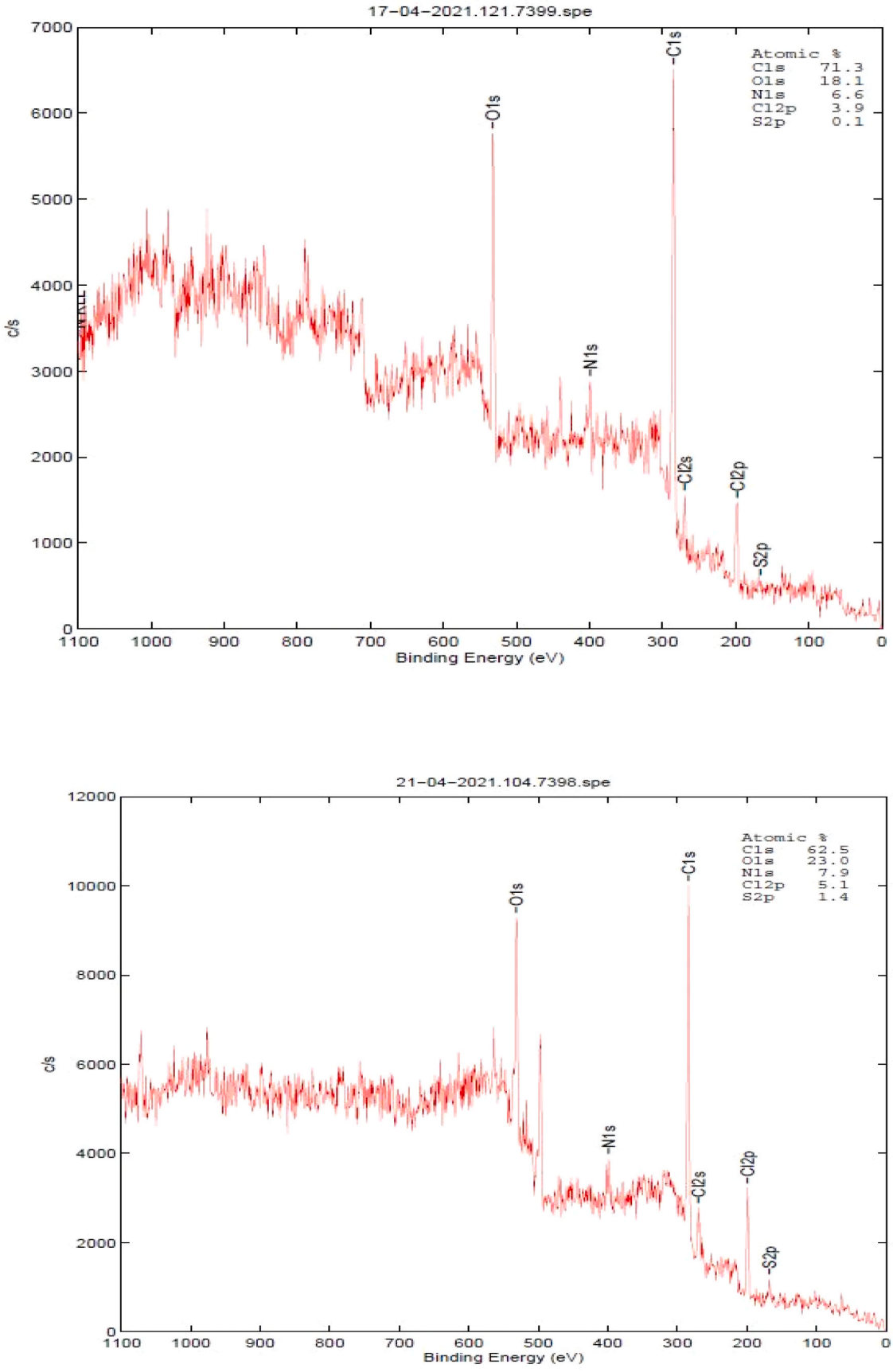


Fig. 4. XPS analysis of synthesized metal based nanocomposite.

and grinded to powder using mixer. 10 g of obtained powder was dissolved in 50 ml of double distilled water and allowed to boil at 60 °C for 1 h. The boiled solution was then filtered using whatmann filter paper and the collected extract was stored at 4 °C for further use.

2.2. Synthesis of TiO_2/Fe_2O_3/Chitosan Nanocomposite

TiO_2 and Fe_2O_3 nanoparticles were synthesized using green synthesis method using titanium tetra isopropoxide and Ferric chloride as precursors respectively. The techniques used here are available in literatures (Shaker Ardakani et al., 2021) (Balaji et al., 2019). The 0.5 g of obtained TiO_2 nanoparticle and 1.5 g of Fe_2O_3 nanoparticles is added to 2 g of chitosan dissolved in 20% acetic acid. The mixture is then homogenized using sonicator for 3 h. Obtained mixture is dried in hot air over at 80 °C for 4 h. The dried mixture is then finely powdered using mortar and pestle and the obtained nanocomposite powder is stored for further studies.

2.3. Characterization of TiO_2/Fe_2O_3/Chitosan Nanocomposite

The obtained nanocomposites were characterized using several methods. The composition of nano- composites was estimated using X-ray photoelectron spectroscopy (XPS) (ULVAC-PHI, Inc; Model: PHI5000 Version Probe III) and XRD (Bruker, D8- Advance). The morphology of nanocomposites was observed using SEM (EVO-18) and Transmission Electron Microscopy (TEM) (FEL-Tecnai G2 20 Twin).

2.4. Sorption experiment for paracetamol removal

Box- Behnken design (BBD) is used for optimizing the factors like pH, Agitation speed and sorbent dosage in paracetamol removal. Experiments were accomplished in 250 ml Erlenmeyer flask. 100 ml of 50 ppm concentration of paracetamol solution is taken. pH, agitation speed and sorbent dosage are adjusted according to the run. After 90 min, solution is filtered using whatmann filter paper. Sorbent is collected and the concentration of paracetamol in the filtrate is analyzed using UV–Visible Spectrophotometer (Shimadzu UV-1700 spectrophotometer) at 243 nm. A schematic diagram of the methodology is depicted in Fig. 1.

The removal percentage of paracetamol is given by

$$\% = \frac{C_o - C_e}{C_o} \times 100 \quad (1)$$

Adsorption capacity (q_e) is calculated by

$$q_e = \frac{(C_o - C_e)V}{m} \quad (2)$$

Where C_o and C_e are initial and final concentration of paracetamol (mg/L), q_e - uptake capacity (mg/g),V - Volume of sample (Solution in ml), m - mass of sorbent (g) (Jayakumar et al., 2021).

3. Results and discussion

3.1. Characterization

3.1.1. Morphological

The surface morphology particle distribution of the sample was further characterized through SEM and TEM analysis. Fig. 2a shows the SEM image of TiO_2-Fe_2O_3-chitosan sample, which shows the irregular shaped nanoparticles with agglomerations. The particles like TiO_2 and Fe_2O_3 are folded by the rough and irregular shaped chitosan with slight porosity which is further confirmed by the TEM images. Fig. 2b shows the high resolution TEM images of TiO_2-Fe_2O_3-chitosan sample. TEM image (Fig. 2b) also shows the rough and irregular shape which is aroused from the factor of chitosan (Dark colour). Also, Fig. 2c shows the high resolution TEM image of TiO_2-Fe_2O_3-chitosan nanoparticles, which illustrates the amorphous nature of the nanocomposite. As from these result, the roughness and porosity nature of the sample can enhance the catalyst performance during the degradation or adsorption process.

Table 1
Factor levels for sorptive removal of Paracetamol.

Variables	Code	Levels		
		−1	0	1
pH	A	4	6	8
Agitation Speed, (rpm)	B	100	200	300
Sorbent Dosage (g/l)	C	0.1	0.5	0.9

Table 2
BBD and sorptive removal of paracetamol Using TiO_2/Fe_2O_3/Chitosan Nanocomposite.

Run Order	A	B	C	% Removal of Paracetamol	
				Experimental	Predicted
1	0.00	1.00	1.00	77.72	74.61
2	0.00	0.00	0.00	74.39	75.43
3	−1.00	0.00	1.00	56.70	57.88
4	1.00	1.00	0.00	87.13	85.23
5	0.00	0.00	0.00	76.79	75.43
6	−1.00	−1.00	0.00	51.78	53.68
7	−1.00	1.00	0.00	53.09	55.03
8	0.00	0.00	0.00	75.12	75.43
9	−1.00	0.00	−1.00	59.63	54.62
10	0.00	−1.00	−1.00	61.12	64.23
11	1.00	0.00	0.00	90.59	95.60
12	1.00	0.00	−1.00	80.23	79.05
13	0.00	−1.00	1.00	78.79	75.72
14	1.00	−1.00	0.00	87.57	85.63
15	0.00	1.00	−1.00	63.21	66.29

3.1.2. Thermogravimetric analysis (TGA)

The stability of the synthesized nanocomposite was evaluated using TGA. TGA analysis was performed and it is illustrated in Fig. 3a and b. From the figures, it has been concluded that a decrease in weight occurs in 3 stages. It shows 8.859% weight loss in the temperature range of 40–150 °C. This may be due to the removal of observed moisture in the nanocomposite. A further increase in temperature from 150 to 350 °C, a strong dip is observed with a loss of 34.09%. From 350 to 800 °C, the loss is found to be 24.31%.

Differential scanning calorimetry (Fig. 3b) was employed with N_2 (30 - 800°C) at a heating rate of 20°C/min. A peak at 86.8 °C indicates the glass transition temperature of $FeCl_3$ used as dopant during synthesis of nanocomposite.

3.1.3. XPS

Wide survey spectrum obtained from X-ray photoelectron spectroscopy (XPS) of nanocomposite before adsorption shows six major peaks (Fig. 4) that possess binding energies of C 1s, N 1s, O 1s, Cl 2_S Cl 2p and S 2p at eV respectively. The spectrum indicates the presence of C, N, O, Fe and S. The peaks at the binding energy of 300, 290 and 200 eV correspond to C 1s, Cl 2s and Cl 2p respectively. The binding energy of Cl 2s and Cl 2p at 290 and 200 eV assigned to chlorine atom which can be generated from $FeCl_3$ used during synthesis of nanocomposite. The peak at binding energy of 170 eV corresponds to S 2p. The peak at binding energy of 400 eV corresponds to N 1s shows the presence of amines, imines and positively charged nitrogen atoms. The peak at binding energy of 540 eV corresponds to O 1s which corresponds to lattice oxygen and surface oxygen. The presence of peak at 300 eV corresponding to C 1s confirms the presence of carbon in the composite which is supposed to be major element of chitosan compound. The peak at binding energy of 400 eV corresponding to N 1s proves that chitosan is present in the composite since nitrogen is also component of chitosan. The peak at

Table 3
ANOVA for paracetamol removal using TiO_2/Fe_2O_3/chitosan nanocomposite.

Source	Sum of Squares	df	Mean Square	F-value	P-value
Model	2410.13	9	267.79	6.97	0.0229
A	1931.93	1	1931.93	50.27	0.0009
B	9.37	1	9.37	0.24	0.6423
C	300.86	1	300.86	7.83	0.0381
AB	0.76	1	0.76	0.02	0.8933
AC	44.16	1	44.16	1.15	0.3328
BC	9.89	1	9.89	0.25	0.6335
A^2	1.62	1	1.62	0.04	0.8453
B^2	87.86	1	87.86	2.29	0.1910
C^2	32.85	1	32.85	0.85	0.3976
Residual	192.17	5	38.43		
Lack of Fit	189.14	3	63.05	41.65	0.0235
Pure Error	3.03	2	1.51		
Cor Total	2602.30	14			

Std. Dev-4.67; R^2 -0.9536; Mean - 71.59; Adj R^2- 0.8700; C.V. % - 6.52; Pred R^2 - 0.2750; PRESS-1702.61; Adeq Precision- 10.996.

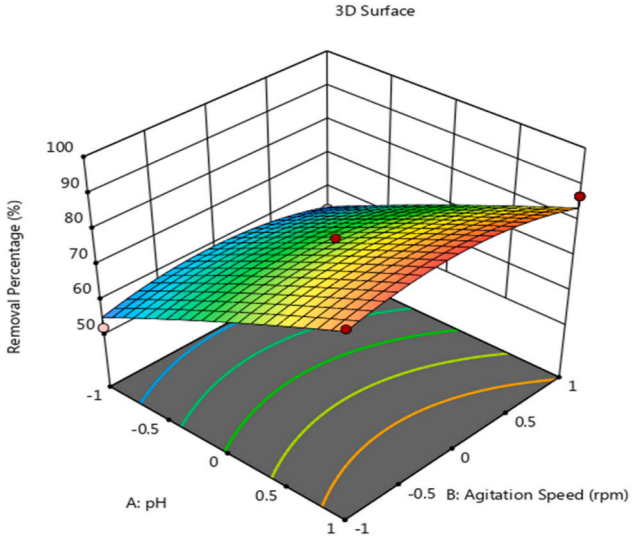


Fig. 5. Effect of pH and agitation speed on Paracetamol sorption.

binding energy of 540 eV corresponding to O 1s reveals the presence of oxides of titanium and ferrous in the composite. The peak at 780 eV assigned to Fe 2p confirms that ferrous is also constituent of composite. The shift in the peaks of C 1s, N 1s and O 1s witnesses that materials are binded in composite and responsible adsorption of paracetamol.

3.2. Sorption experiments

According to Box Behnken Design (Tables 1 and 2), the sorption study for the paracetamol was carried out using nanocomposite. The results obtained in sorption study was represented in Table 2.

The expression for the response of the sorption study among the variables is given by the following equation (3)

$$\text{Removal of paracetamol, \%} = 75.433 + 15.54A + 0.24B + 4.95C - 0.44AB + 3.32AC - 0.79BC - 1.98A^2 - 3.56B^2 - 1.66C^2 \quad (3)$$

Where A, B and C are the coded values of pH, agitation speed (rpm) and sorbent dosage (g/l).

The results obtained in sorption study is illustrated in ANOVA which was represented in Table 3. Based on the results, the model was found to be significant with the F value of 6.97 and P value less than 0.5. Among the three terms A, B and C, the significant term is A and C. When compared to the percentage of removal between experimental and predicted one, the experimental results are compatible with the

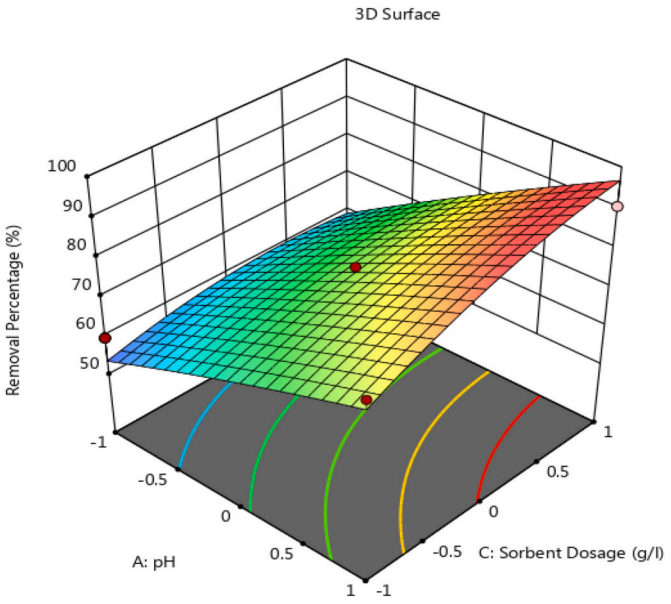


Fig. 6. Effect of pH and Sorbent dosage on Paracetamol sorption.

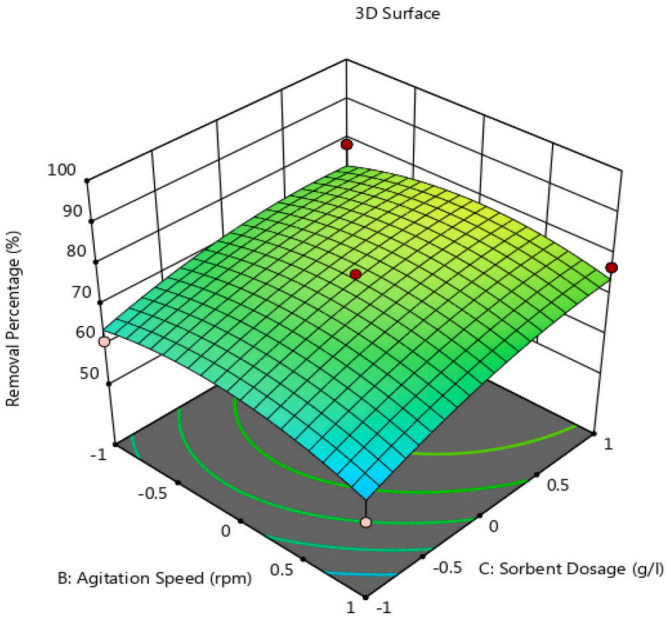


Fig. 7. Effect of agitation speed and Sorbent dosage on Paracetamol sorption.

predicted one. As the coefficient of variance is low which indicates that the deviation between the values of predicted and the experimental one is also low.

3.2.1. Effect of factors on Paracetamol removal

Removal of Paracetamol depends on various factors like pH, agitation speed, sorbent dosage. The effect of pH on paracetamol sorption on to nanocomposites is examined by varying the pH from 4.0 to 8.0. The results are depicted in Fig. 5. It is clear from the figure that, the pH has great influence on the sorption of paracetamol. The pH influences surface properties of the nanocomposites by the way of functional group dissociation and surface charges. At pH 4 removal of paracetamol is found to be very low. This indicates that removal of paracetamol is not favorable under acidic conditions. Removal of paracetamol is found to increase with increase in pH and it was maximum at the pH of 7.5. Therefore, the pH 7.5 is adjusted with 0.1 N NaOH for further

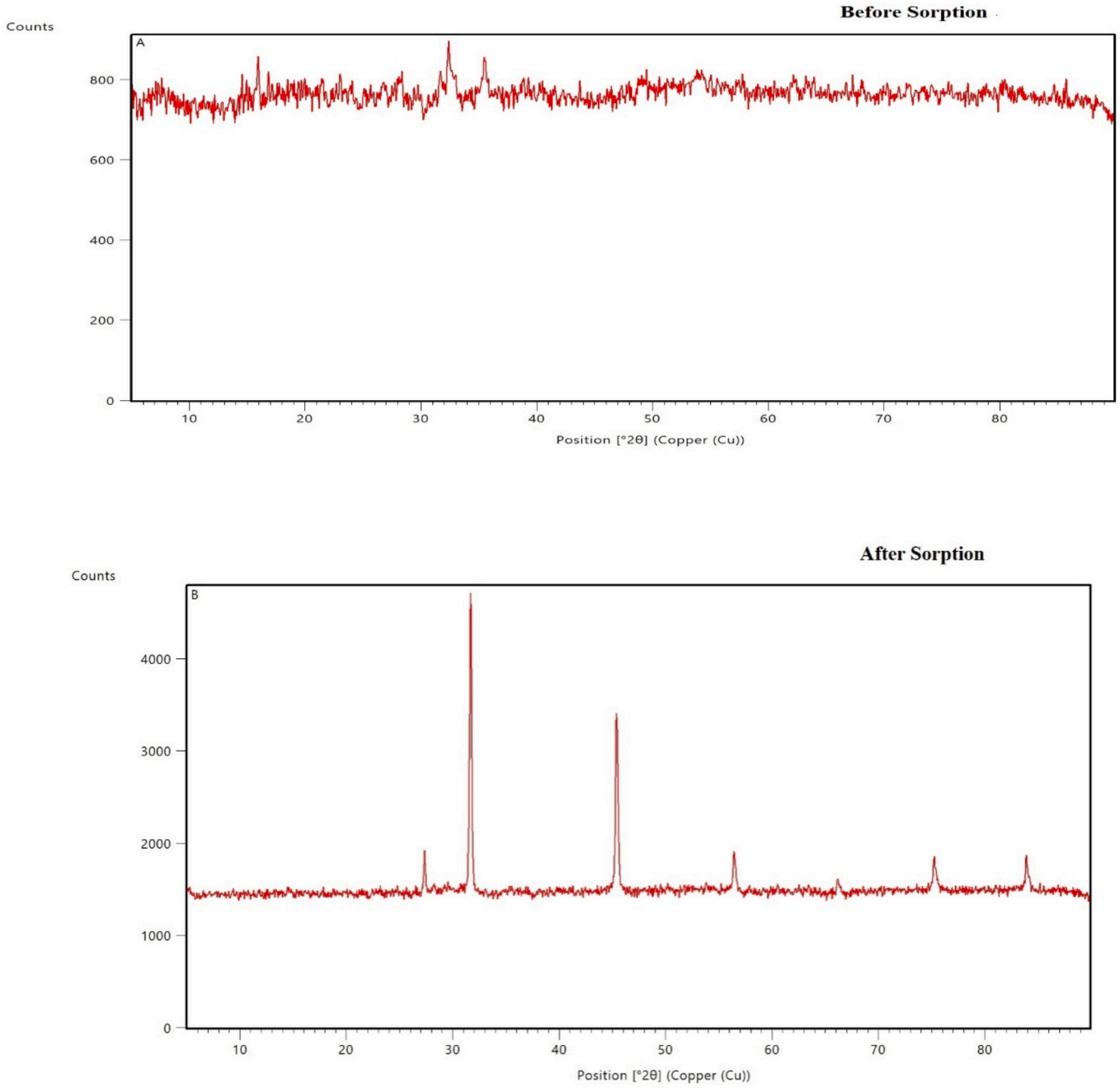


Fig. 8. a and b X-Ray Diffraction patterns of TiO_2/Fe_2O_3/Chitosan nanocomposite before and after sorption.

experiments. A decrease in sorption capacity of paracetamol at pH less than 7 was possibly due to the formation of paracetamol dimers in the solution and to the repulsions between the sorbent surface having positive charges as well as the carbocation of paracetamol. As the sorption capacity is low at less solution pH, it can be confirmed that the donor-acceptor electron mechanism is less active (Bernal et al., 2017).

The effect of sorbent dosage on removal of paracetamol is studied by changing the sorbent dosage from 0.1 to 0.9 g/l. The results obtained are shown in Fig. 6. Maximum removal of paracetamol is obtained at 0.5 g/l of sorbent dosage. The reason is, the increase in dosage creates a large contact surface area which in turn produces large amount of vacant sites but the available sorbate are limited. Previous literatures on the application of nanocomposites (Sarojini et al., 2021; Karimi et al., 2012) reported similar results for the removal of pollutant by adsorption process. At the optimum conditions the experiments are performed and maximum removal of 90.59% is achieved.

The effect of agitation speed is examined in the range of 100–300 rpm and it is depicted in Fig. 7. From the figure, it has been found that the maximum removal of paracetamol occurs at 200 rpm. The percentage of removal is less at low speed because of the sorbent deposition at the bottom. Then adsorption capacity of the sorbent reduced and attained equilibrium at 250 rpm. This is in accordance with many literatures (Rajamohan et al., 2014; Sarojini et al., 2021).

3.3. Sorbent characterization after sorption

3.3.1. XRD

Phase and crystalline nature of the prepared samples were utilized through XRD analysis. Nature of the nanocomposite can be analyzed using XRD (Rajamehala et al., 2022). Fig. 8a and b shows the XRD

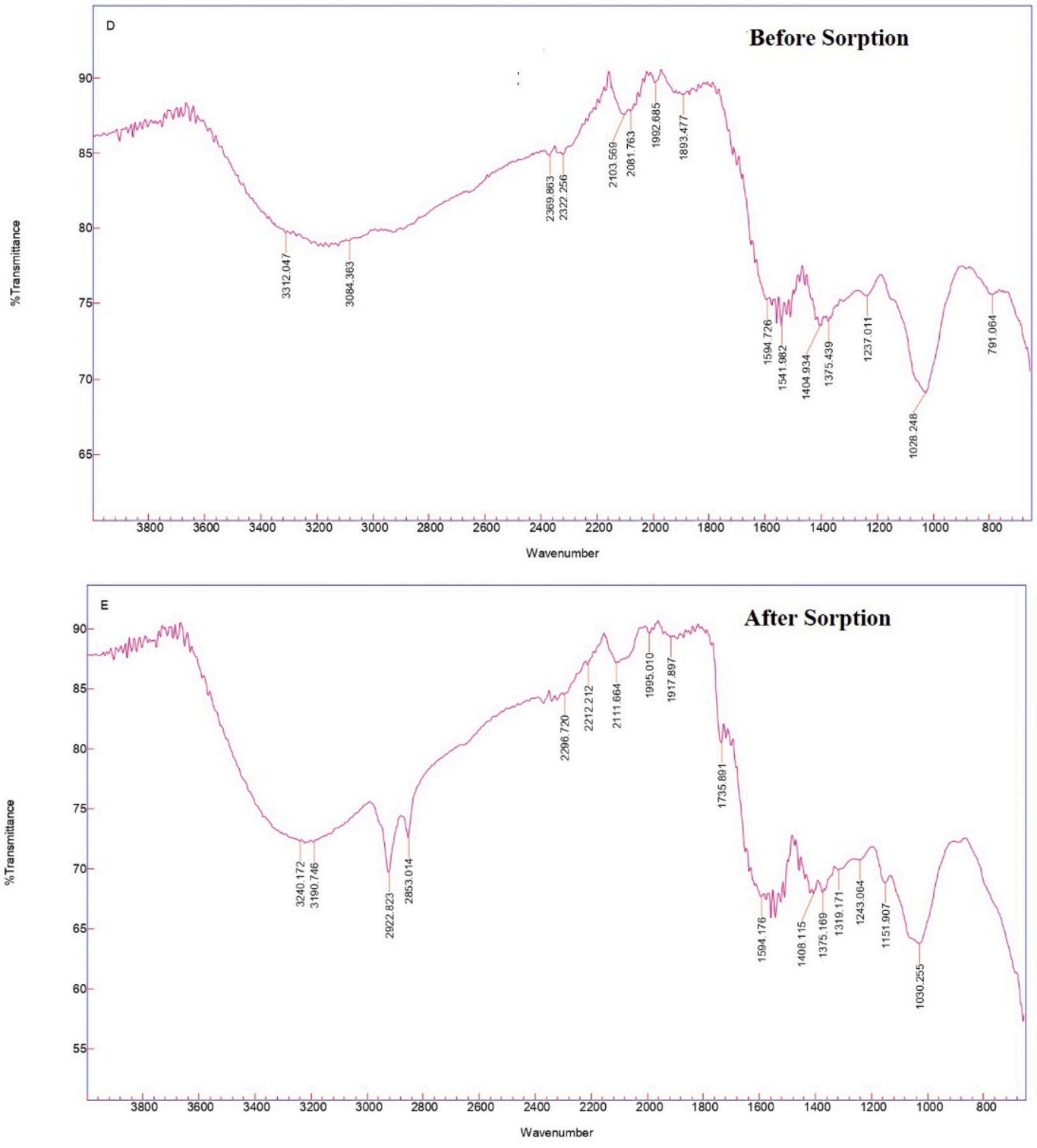


Fig. 9. FTIR of nanocomposite before and after sorption.

spectra of synthesized TiO_2-Fe_2O_3-chitosan sample. X-ray powder diffraction technique verified inadequate distinguishing diffraction peaks throughout the pattern demonstrating the amorphous nature of the synthesized nanocomposites. The main diffraction peaks of 2Θ at 18, 30, 48, showed the presence of Chitosan, TiO_2 and Fe_2O_3 nanoparticles. No sharp peaks were observed. After adsorption, sharp peaks were observed indicating crystalline form. The change in diffractogram indicates that adsorption of paracetamol altered the phase of nanocomposite.

3.3.2. *FTIR*

FTIR measurements of the nano sorbent are performed to ascertain the functional groups present in it. The FTIR spectra of TiO_2/Fe_2O_3/ Chitosan Nanocomposite before and after sorption was presented in

Table 4
FTIR of nanocomposite before and after sorption of paracetamol.

Wavelength Range (cm^{-1})	TiO_2/Fe_2O_3/Chitosan Nanocomposite		Functional Groups
	Before Sorption	After Sorption	
3500–3000	3312.047	3240.172	Bonded–OH groups
	3084.363	3190.746	Bonded–OH groups
3000–2800	–	2922.823	CH stretching
	–	2853.014	CH stretching
2400–2000	2103.569	2296.720	N=C=S stretching
	2081.763	2212.212	C (triple bond) N stretching
	–	2111.664	C (triple bond) C stretching
2000–1650	1992.685	1995.010	CH bending
	1893.477	1917.897	CH bending
	–	1735.891	C=O stretching
1600–1300	1594.726	1594.176	
	1541.982	–	N–O stretching
1400–700	1404.934	1408.115	O–H bending
	1375.439	1375.169	O–H bending
	1237.011	1234.064	C–O stretching
	1028.248	1151.907	C–N stretching
	–	1030.255	S=O stretching
	791.064		C=C bending

Table 5
Isotherms used for the sorption of paracetamol.

Isotherm	Non-Linear form	Linear form	Reference
Langmuir	$q_{e=}\frac{q_m b C_e}{1+bC_e}$	$\frac{1}{q_e}=\frac{1}{q_m}+\frac{1}{q_m b C_e}$	Langmuir (1916)
Freundlich	$q_{e=}K_f C_e^{1/n}$	$log\ q_{e=}\ log\ K_f + \frac{1}{n}\log C_e$	Freundlich, 1906
Dubinin-Radushkevich (DR)	$q_{e=}q_s \exp(-k_{ad}\in^2)$	$ln\ q_{e=}\ ln\ q_s - k_{ad}\in^2$	Dubinin (1960)
Temkin	$q_{e=}\frac{RT}{b_T} ln\ A_T C_e$	$q_{e=}\frac{RT}{b_T} ln\ A_T + \frac{RT}{b_T} ln\ C_e$	Temkin and Pyzhev, 1940

Table 6
Isotherm model parameters for Paracetamol sorption on to TiO_2/Fe_2O_3/Chitosan Nanocomposite.

Isotherm	Parameters			
	Linear		Non-Linear	
Langmuir	q_{max}	175.4386	q_{max}	178.1
	B	0.372	B	0.3392
	R^2	0.9973	R^2	0.9755
Freundlich	K_f	55.55	K_f	72.2
	1/n	0.3321	n	4.193
	R^2	0.9247	R^2	0.9018
D-R	q_{max}	143.33	Kdr	155.2
	B	0.3798	Bdr	1.213
	E	1.147	R	1.494
	R^2	0.909	T	1.323
			R^2	0.8229
Temkin	B	32.786	R	1.702
	K_T	5.012363	T	1.258
			Br	0.06829
	R^2	0.9746	A_T	6.133
			R^2	0.9575

Fig. 9. The major zones observed in the transmittance spectrum correspond to Carboxylic, alkane, alkene, alkyl and hydroxyl functional groups. The band shows the presence of broad adsorption band between 3500 and 3000 cm^{-1} due to the O–H stretching and H- bonded alcohols and phenol groups. The bands between 2400 and 2000 cm^{-1} correspond to N=C=S stretching and primary amine, CN stretching vibrations respectively. The vibration modes of Ti–O in the nanocomposite cause the characteristic peak at 1375 cm^{-1}. The N–H scissoring from the primary amine due to the free amino groups in the cross-linked chitosan is confirmed by the peaks about 2000–1650 cm^{-1}. (Bhanvase et al., 2019). The shifting of peaks after sorption is also presented in Table 4. Substantial modifications are detected in the peak values, which specify the physical interaction between paracetamol and nanocomposite. This shift in peak values may be due to the formation of chemical bond between functional groups present on nanocomposite and paracetamol. Similar shift in peaks is noted in Lung et al. (2021).

3.4. Equilibrium and isotherm studies

The different adsorption isotherms are used to study the paracetamol adsorption performance and were given in the Table 5.

The experimental data are fitted with both linear and non-linear models of Langmuir, Freundlich, D-R, Temkin isotherms and the parameters are given in the Table 6.

The Langmuir isotherm is based on regularity and homogeneity of the sorbent and binds to a surface with numerous vacant sites for single layer sorption. The model's main flaw is that, it assumes adsorbents at each site have uniform energies.

The R_L determines the isotherm's favorability, which should be less than one for fitness.

$$R_{L=\frac{1}{1+(1+bC_o)}} \quad (4)$$

where C_o - initial concentration of paracetamol.

The correlation coefficient value of above 0.90 shows the fitness of experimental data with model prediction. It is observed that high correlation is observed in both linear (R^2 = 9973) and non-linear (R^2 = 9755) models of Langmuir isotherm. Results show that the proper nature of the above-mentioned isothermal model indicates that an adsorption process homogenous. The Freundlich isotherm constant value of 1/n, between 0 and 1, indicates good adsorption. Here (1/n) = 0.3321 suggests that the sorption of paracetamol was favorable.

Hence, Langmuir adsorption isotherm is favorable for experimental data for the sorption of paracetamol using TiO_2/Fe_2O_3/Chitosan nanocomposite.

The Temkin isotherm's high R^2 value indicates that the model fits the data well. Physical adsorption occurs in the D-R isotherm when E is less than 8 kJ/mol, whereas chemical adsorption occurs only when E is greater than 8 kJ/mol (Sarojini et al., 2021). The table revealed that E = 1.147, indicating that the process was physical. Based on the findings, it is possible to conclude that the sorption mechanisms tend to follow the Langmuir model. This is also clearly depicted in Fig. 10.

3.5. Kinetic studies

Kinetics is vital for an effective implications of pollutant removal on sorbent because it allows us to understand the mechanism of adsorption and potential rate-limiting steps. Furthermore, knowledge on the kinetics of pollutant absorption is required in order to select the best conditions for the full-scale batch pollutant removal process. Different kinetic models are employed in order to analyze the adsorption rate of paracetamol on to TiO_2/Fe_2O_3/Chitosan Nanocomposite.

3.5.1. Pseudo First Order Model

Lagergren proposed a pseudo-first-order equation (Yuh-Shan, 2004) and in linear form it is:

$$\log(q_e - q_t) = \log q_e - \frac{K_l}{2.303} t \quad (5)$$

Where q_t and q_e (mg/g) are the amount of the pollutant adsorbed at time

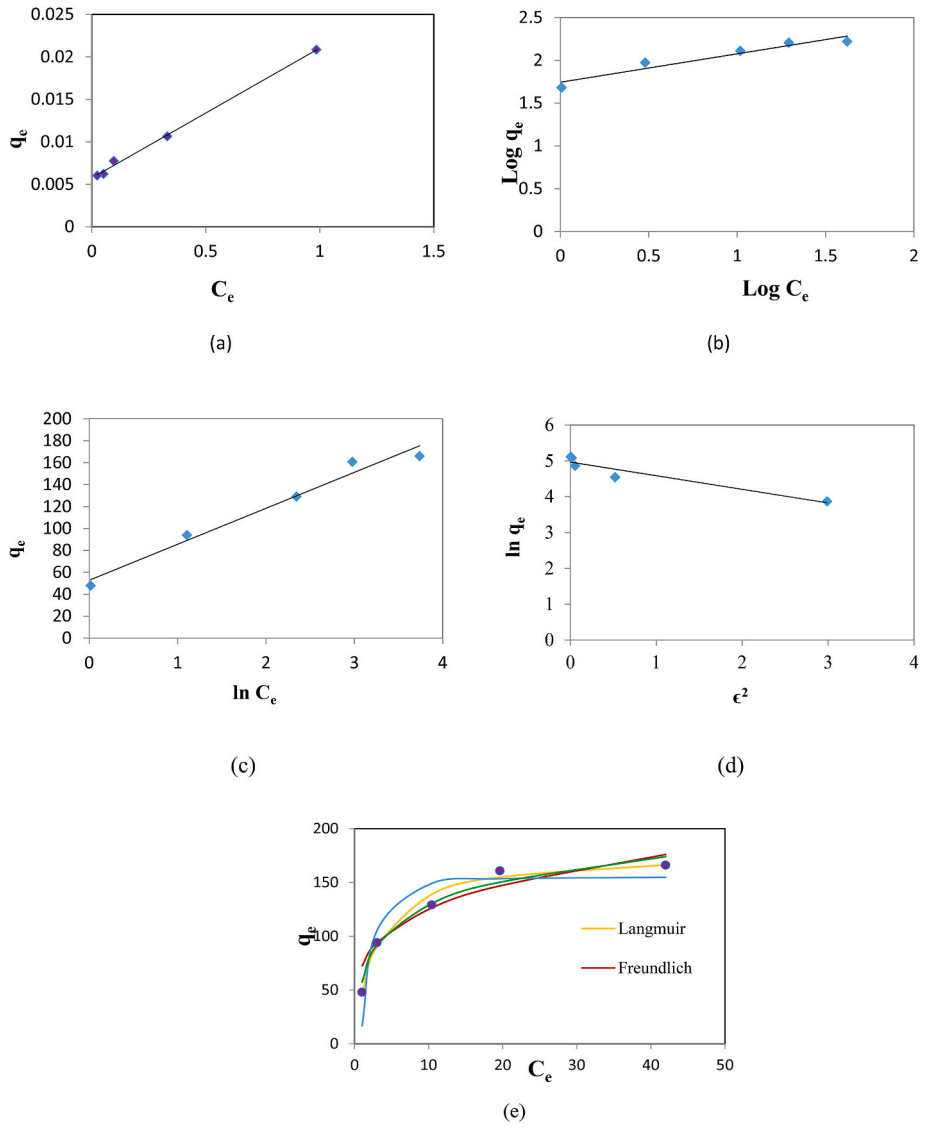


Fig. 10. Isotherm models: (a) Langmuir isotherm (b) Freundlich isotherm (c) Temkin isotherm (d) D-R isotherm (e) non- linear model.

t (min) and equilibrium (mg/g), respectively. K_1 is the rate constant of the equation (min^{-1}) (Vasudevan et al., 2010). The coefficient determination of pseudo first order is 0.9481 and value of rate constant K_1 is calculated as 0.02786 min^{-1}.

3.5.2. Pseudo second order model

The sorption behavior over the whole adsorption time is predicted by the pseudo second order model (Ho and McKay, 1999)

$$\frac{t}{q_t} = \frac{1}{K_2 q_e^2} + \frac{1}{q_e} t \tag{6}$$

Where K_2 (g/mg min) is the rate constant of the second order equation. q_t and q_e (mg/g) are the amount of the pollutant adsorbed at time t (min) and equilibrium (mg/g) (Kamaraj et al., 2016, 2018; Kamaraj and Vasudevan, 2016). From the plot it is calculated that coefficient of Pseudo second order reaction is 0.4531 and K_1 is 0.0000057 g/mg.min.

3.5.3. Intra Particle Diffusion model

In order to understand the transport phenomena on adsorption of liquid particles onto the solid support, diffusion study was carried out (Weber and Morris, 1963), which is given by the following equation:

Table 7
Kinetic Parameters for the sorption of paracetamol.

Kinetic Model	Parameters for Paracetamol	
I Order	K_1 (min^{-1})	0.02786
	R2	0.9481
II Order	K_2 (g/mg min)	0.0000057
	R2	0.4531
Intra Particle Diffusion	K_{id} (mg/g $min^{0.5}$)	10.756
	R2	0.8798
Elovich	α (mg/g min)	3.40
	β(g/mg)	0.0198
	R2	0.9818

$$q_t = K_{id} t^{0.5} + C \tag{7}$$

Where K_{id} is the intraparticle diffusion rate constant (mg/g $min^{0.5}$) and C is the intercept.

3.5.4. Elovich Model

The Elovich model (Ozacar and Sengil, 2005) integrates α as the initial adsorption rate (mg/g min) and β as the desorption constant. A plot of q_t vs ln(t) should give a linear relationship with a slope of (1/β)

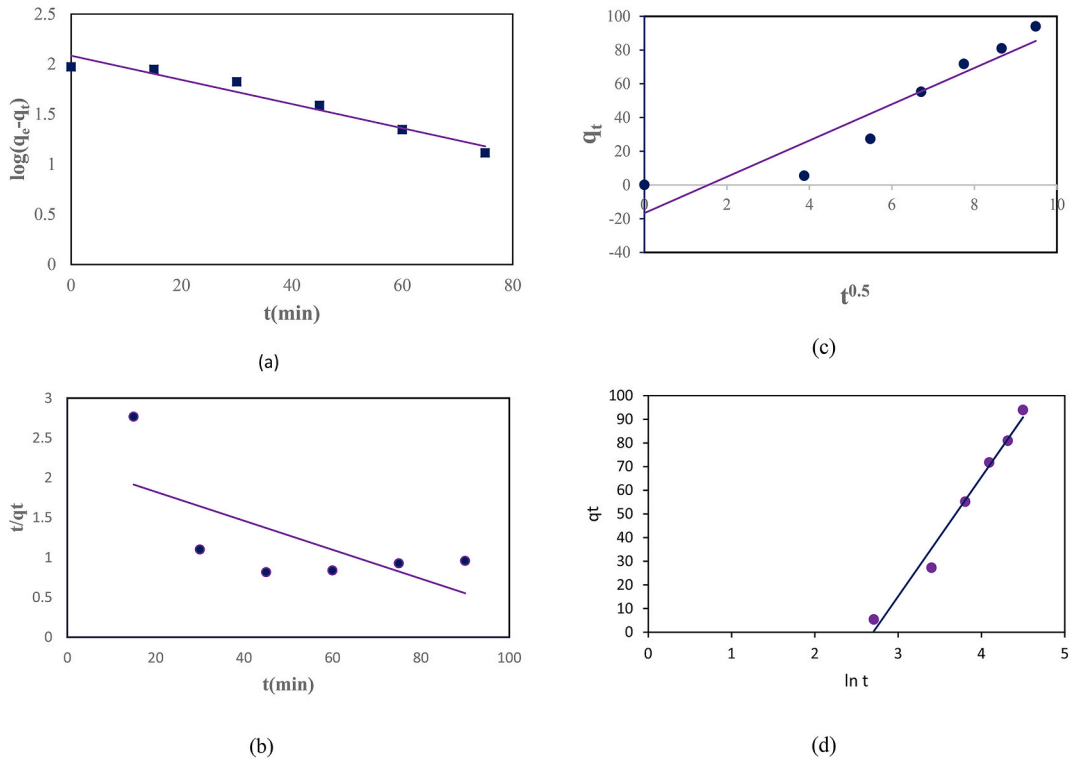


Fig. 11. Kinetic Models: a) Pseudo First Order b) Pseudo Second Order c) Intra Particle Diffusion (d) Elovich Model.

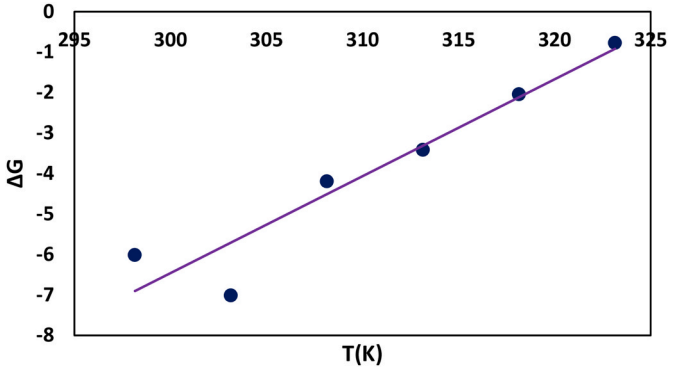


Fig. 12. Thermodynamic plot for the sorption of paracetamol.

and an intercept of (1/β) ln(αβ)

$$q_t = \frac{1}{\beta}\ln(\alpha\beta) + \frac{1}{\beta}\ln t \tag{8}$$

where α - constant of Elovich model (mg/g^{-} min) and β - exponent in Elovich model (g/mg).

The values of the kinetic model parameters are presented in Table 7

Table 8
Thermodynamic parameters for Paracetamol sorption on to TiO_2/Fe_2O_3/Chitosan Nanocomposite.

Pollutant	Temp(K)	ΔG^o (kJ/mol)	ΔS^o (kJ/mol K)	ΔH^o (kJ/mol)
Paracetamol	298.15	−6.0161	0.2395	78.297
	303.15	−7.0143		
	308.15	−4.1942		
	313.15	−3.4152		
	318.15	−2.0445		
	323.15	−0.7727		

and plots are presented in Fig. 11. From these figures, it is observed that the Pseudo first order, intra particle and Elovich kinetic models fit the experimental data very well. The R^2 greater than 0.89 shows the validity of these model. Based on the correlation coefficient, the Elovich model best fits the sorption of paracetamol when compared to other models.

3.6. Thermodynamic studies

The effect of temperature on paracetamol removal is studied between 298.15 K and 323.15 K and is depicted in Fig. 12. Adsorption removal efficiency initially increases with increasing temperature due to increased particle movement and was found to be maximum at 303.15 K. At this temperature, the molecules should have enough energy to interact on the free sites on the nanocomposite surface. Further temperature variations have little effect on sorption efficiency. A decrease in paracetamol removal was observed at very high temperature 323.15 K. It implies that higher temperatures seem to be not suitable for Paracetamol adsorption using the produced nanocomposites. Furthermore, increasing the temperature increases the adsorbate mobility, resulting in desorption, and the interaction between Paracetamol and nanocomposite was exothermic at higher temperatures.

Thermodynamic aspects for sorption of paracetamol on nanocomposite is found using the following equations:

$$\Delta G = RT\ \ln K \tag{9}$$

$$\Delta G = \Delta H - T\Delta S \tag{10}$$

Where R-Universal Gas Constant (8.314×10^{-3} kJ/mol K)

T - Temperature in Kelvin and
K - Equilibrium constant,

$$K = \frac{q_e}{C_e} \tag{11}$$

ΔG - Gibbs free energy (kJ/mol)

Table 9
Comparative Study on removal of paracetamol using different sorbents.

Adsorbent	Adsorption capacity (mg/g)	Reference
Clay-based, activated carbon, cement, and PVA polymer composite	14.67	Ait Hamoudi et al. (2021)
Rice Husk	50	Lahieb et al. (2020)
Activated Carbon from coffee grounds	50	Benyekkou et al. (2020)
natural Jordanian zeolite	55.6	Al-rimawi et al. (2019)
Fe3O4@C matrix	141.9	Moacă et al. (2019)
Agricultural waste (oak acorn)	45.45	Nourmoradi et al. (2018)
Activated carbon derived spent tea leaves	59.2	Wong et al. (2018)
Activated carbon cloths	105	Boudrahem et al. (2017)
Rice Hull Activated carbon	169.49	Mupa (2015)
activated carbon of Babassu Coconut Mesocarp	71.39	Ferreira et al. (2015)
TiO_2/Fe_2O_3/Chitosan Nanocomposite	175.43	Current Study

ΔH - Enthalpy change (kJ/mol) and
ΔS -Entropy change (kJ/mol K).

The values of ΔH and ΔS are found using from the intercept and slope of the graph, ΔG versus T for paracetamol sorption using TiO_2/Fe_2O_3/Chitosan nanocomposite (Jayakumar et al., 2021). The values of these parameters are presented in Table 8 (Sahmoune, 2019). The positive value of ΔH indicates that the sorption is endothermic, and the positive value of ΔS indicates that the randomness at the solid-solution interface increases during the sorption process. ΔG with a negative value indicates that the sorption process was spontaneous, whereas ΔG with a positive value indicates that the sorption process was favorable (Mohammed et al., 2018).

A comparison has been made for paracetamol removal using other sorbents and it is provided in Table 9. It can be seen that the nanocomposite synthesized in this work show good uptake of paracetamol when compared to others.

4. Conclusion

An attempt has been made to remove pharma pollutant concerning the use of a novel nanocomposites synthesized from *Moringa olifera* extract rather than commercial activated carbon. The adsorption characteristics of synthesized nanocomposite to remove paracetamol have been studied, with emphasis on uptake, kinetics, equilibrium and thermodynamics. The adsorption data were fitted to the Langmuir isotherm model, with R^2 values of 0.9973 and the maximum monolayer adsorption capacities of 175.43 mg/g for paracetamol, which is very high when compared to other literatures. Furthermore, the kinetic studies corresponded well to the pseudo-first-order kinetic model. The sorption process was found to be spontaneous, endothermic, and physical. The findings confirmed the efficacy and applicability of nanocomposite in the treatment of aquatic systems contaminated with NSAIDs like paracetamol. The findings of this study indicated that a green-synthesized nano-adsorbent could be used as a promising resource to efficiently remove pollutants generated from pharmaceutical industries in a real time manner in the future.

Author contributions

M. Rajamehala - Conceptualization, Data curation, Investigation, Validation, Software, Visualization, Writing – original draft. **A. Muthukumara Pandian -** Resources, Formal analysis, Software, Supervision, Writing – Review & Editing. **M. Rajasimman -** Resources, Methodology, Writing – Review & Editing. **B. Gopalakrishnan -** Methodology, Supervision, Validation, Writing – Review & Editing.

Declaration of competing interest

The authors declare that they have no known competing financial interests or personal relationships that could have appeared to influence the work reported in this paper.

Data availability

Data will be made available on request.

References

Ait Hamoudi, S., Brahimi, M., Boucha, M., Hamdi, B., Arrar, J., 2021. Removal of paracetamol from aqueous solution by containment composites. Open Chem. 19, 49–59. https://doi.org/10.1515/chem-2020-0188.

Al-rimawi, F., Daana, M., Khamis, M., Karaman, R., Khoury, H., Qurie, M., 2019. Removal of selected pharmaceuticals from aqueous solutions using natural Jordanian zeolite. Arabian J. Sci. Eng. 44, 209–215. https://doi.org/10.1007/s13369-018-3406-9.

Balaji, S., Guda, R., Mandal, B.K., Kasula, M., Ubba, E., Khan, F.R.N., 2019. Green synthesis of nano-titania (TiO 2 NPs) utilizing aqueous Eucalyptus globulus leaf extract: applications in the synthesis of 4H-pyran derivatives. Res. Chem. Intermed. https://doi.org/10.1007/s11164-018-03720-0.

Benyekkou, N., Ghezzar, M.R., Abdelmalek, F., Addou, A., 2020. Elimination of paracetamol from water by a spent coffee grounds biomaterial. Environ. Nanotechnol. Monit. Manag. 14, 100396 https://doi.org/10.1016/j.enmm.2020.100396.

Bernal, V., Erto, A., Giraldo, L., Pirajan, J.C.M., 2017. Effect of solution pH on the adsorption of paracetamol on chemically modified activated carbons. Molecules 22 (2017), 1032. https://doi.org/10.3390/molecules22071032.

Bhanvase, B.A., Veer, A., Shirsath, S.R., Sonawane, S.H., 2019. Ultrasound assisted preparation, characterization and adsorption study of ternary chitosan-ZnO-TiO2 nanocomposite: advantage over conventional method. Ultrason. Sonochem. 52, 120–130. https://doi.org/10.1016/j.ultsonch.2018.11.003.

Blackburn, R.S., 2004. Natural polysaccharides and their interactions with dye molecules: applications in effluent treatment. Environ. Sci. Technol. 38, 4905–4909. https://doi.org/10.1021/es049972n.

Boudrahem, N., Delpeux-Ouldriane, S., Khenniche, L., Boudrahem, F., Aissani-Benissad, F., Gineys, M., 2017. Single and mixture adsorption of clofibric acid, tetracycline and paracetamol onto Activated carbon developed from cotton cloth residue. Process Saf. Environ. Protect. 111, 544–559. https://doi.org/10.1016/j.psep.2017.08.025.

Candido, J.P., Andrade, S.J., Fonseca, A.L., Silva, F.S., Silva, M.R.A., Kondo, M.M., 2017. Ibuprofen removal by heterogeneous photocatalysis and ecotoxicological evaluation of the treated solutions. Environ. Sci. Pollut. Res. Int. https://doi.org/10.1007/s11356-017-8623-3.

Chandrashekar Kollarahithlu, S., Balakrishnan, R.M., 2021. Adsorption of pharmaceuticals pollutants, Ibuprofen, Acetaminophen, and Streptomycin from the aqueous phase using amine functionalized superparamagnetic silica nanocomposite. J. Clean. Prod. 294, 126155 https://doi.org/10.1016/j.jclepro.2021.126155.

Ciesielski, W., Lii, C., Yen, M.-T., Tomasik, P., 2003. Interactions of starch with salts of metals from the transition groups. Carbohydr. Polym. 51, 47–56.

Crini, G., 2006. Non-conventional low-cost adsorbents for dye removal: a review. Bioresour. Technol. 97, 1061–1085. https://doi.org/10.1016/j.biortech.2005.05.001.

Dubinin, M.M., 1960. The potential theory of adsorption of gases and vapors for adsorbents with energetically nonuniform surfaces. Chem. Rev. 60, 235–241. https://doi.org/10.1021/cr60204a006.

Ferrari, B., Paxéus, N., Giudice, R. Lo, Pollio, A., Garric, J., 2003. Ecotoxicological impact of pharmaceuticals found in treated wastewaters: study of carbamazepine, clofibric acid, and diclofenac. Ecotoxicol. Environ. Saf. 55, 359–370. https://doi.org/10.1016/S0147-6513(02)00082-9.

Ferreira, R.C., de Lima, H.H.C., Cândido, A.A., Junior, O.M.C., Arroyo, P.A., Gauze, G.F., Carvalho, K.Q., Barros, M.A.S.D., 2015. Adsorption of paracetamol using activated carbon of dende and babassu coconut mesocarp. Int. J. Biol. Biomol. Agric. Food Biotechnol. Eng. 9, 575–580.

Freundlich, H.M.F., 1906. Over the Adsorption in Solution. J. Phys. Chem. 57, 385–471.

Hinson, J.A., Reid, A.B., McCullough, S.S., James, L.P., 2004. Acetaminophen-induced hepatotoxicity: role of metabolic activation, reactive oxygen/nitrogen species, and mitochondrial permeability transition. Drug Metab. Rev. 36, 805–822. https://doi.org/10.1081/dmr-200033494.

Ho, Y.S., McKay, G., 1999. Pseudo-second order model for sorption processes. Process Biochem. 34, 451–465. https://doi.org/10.1016/S0032-9592(98)00112-5.

Jayakumar, V., Govindaradjane, S., Rajasimman, M., 2021. Efficient adsorptive removal of zinc by green marine macro alga caulerpa scalpelliformis –characterization, optimization, modeling, isotherm, kinetic, thermodynamic, desorption and

regeneration studies. Surface. Interfac. 22, 100798 https://doi.org/10.1016/j.surfin.2020.100798.
Kamaraj, R., Vasudevan, S., 2016. Facile one-pot electrosynthesis of Al(OH)3 – kinetics and equilibrium modeling for adsorption of 2,4,5-trichlorophenoxyacetic acid from aqueous solution. New J. Chem. 40, 2249–2258. https://doi.org/10.1039/C5NJ02407B.
Kamaraj, R., Pandiarajan, A., Jayakiruba, S., Naushad, M., Vasudevan, S., 2016. Kinetics, thermodynamics and isotherm modeling for removal of nitrate from liquids by facile one-pot electrosynthesized nano zinc hydroxide. J. Mol. Liq. 215, 204–211. https://doi.org/10.1016/j.molliq.2015.12.032.
Kamaraj, R., Pandiarajan, A., Vasudevan, Sudharshan, Vasudevan, Subramanyan, 2018. Facile one-pot electrosynthesis of zinc hydroxide for the adsorption of hazardous 2-(2-methyl-4-chlorophenoxy) propionic acid (MCPP) from water and its modelling studies. J. Environ. Chem. Eng. 6, 2017–2026. https://doi.org/10.1016/j.jece.2018.03.011.
Karimi, H., Mousavi, S., Sadeghian, B., 2012. Silver nanoparticle loaded on activated carbon as efficient adsorbent for removal of methyl orange. Indian J. Sci. Technol. 5, 2346–2353. https://doi.org/10.17485/ijst/2012/v5i3.3.
Lahieb, F.M., Al-Sharify, Z.T., Farah, F.M., 2020. Role of rice husk as natural sorbent in paracetamol sorption equilibrium and kinetics. IOP Conf. Ser. Mater. Sci. Eng. 870, 12053 https://doi.org/10.1088/1757-899x/870/1/012053.
Langmuir, I., 1916. The constitution and fundamental properties of solids and liquids. Part I. Solids. J. Am. Chem. Soc. 38, 2221–2295. https://doi.org/10.1021/ja02268a002.
Liu, G., Feng, M., Tayyab, M., Gong, J., Zhang, M., Yang, M., Lin, K., 2021a. Direct and efficient reduction of perfluorooctanoic acid using bimetallic catalyst supported on carbon. J. Hazard. Mater. 412, 125224 https://doi.org/10.1016/j.jhazmat.2021.125224.
Liu, Y., Zhu, Q., Tayyab, M., Zhou, L., Lei, J., Zhang, J., 2021b. Single-atom Pt loaded zinc vacancies ZnO–ZnS induced type-V electron transport for efficiency photocatalytic H2 evolution. Sol. RRL 5, 2100536. https://doi.org/10.1002/solr.202100536.
Lung, I., Soran, M.L., Stegarescu, A., Opris, O., Gutoiu, S., Leostean, C., Lazar, M.D., Kacso, I., Silipas, T.D., Porav, A.S., 2021. Evaluation of CNT-COOH/MnO2/Fe3O4 nanocomposite for ibuprofen and paracetamol removal from aqueous solutions. J. Hazard. Mater. 403, 1–15. https://doi.org/10.1016/j.jhazmat.2020.123528.
Mane, S.N., Gadalkar, S.M., Rathod, V.K., 2018. Intensification of paracetamol (acetaminophen) synthesis from hydroquinone using ultrasound. Ultrason. Sonochem. 49, 106–110. https://doi.org/10.1016/j.ultsonch.2018.07.029.
Moacă, E.-A., Mihali, C.-V., Macaşoi, I.-G., Racoviceanu (Băbuţă), R., Şoica, C., Dehelean, C.-A., Păcurariu, C., Florescu, S., 2019. Fe3O4@C Matrix with Tailorable Adsorption Capacities for Paracetamol and Acetylsalicylic Acid: Synthesis, Characterization, and Kinetic Modeling. https://doi.org/10.3390/molecules24091727. Mol.
Mohammed, N.A.S., Abu-Zurayk, R.A., Hamadneh, I., Al-Dujaili, A.H., 2018. Phenol adsorption on biochar prepared from the pine fruit shells: equilibrium, kinetic and thermodynamics studies. J. Environ. Manag. 226, 377–385. https://doi.org/10.1016/j.jenvman.2018.08.033.
Mupa M, M.T., 2015. Preparation of rice hull activated carbon for the removal of selected pharmaceutical waste compounds in hospital effluent. J. Environ. Anal. Toxicol. s7 https://doi.org/10.4172/2161-0525.s7-008.
Nourmoradi, H., Moghadam, K.F., Jafari, A., Kamarehie, B., 2018. Removal of acetaminophen and ibuprofen from aqueous solutions by activated carbon derived from Quercus Brantii (Oak) acorn as a low-cost biosorbent. J. Environ. Chem. Eng. 6, 6807–6815. https://doi.org/10.1016/j.jece.2018.10.047.
Ozacar, M., Sengil, I.A., 2005. A kinetic studies of metal complex dye sorption onto pine sawdust. Process Biochem. 40, 565–572. https://doi.org/10.1016/j.procbio.2004.01.032.
Pişkin, Sabriye, Palantöken, Arzu, Yılmaz, Müge Sari, 2013. Antimicrobial Activity of Synthesized TiO2 Nanoparticles, pp. 8–11. https://doi.org/10.15242/IIE.E1213004.
Rabiet, M., Togola, A., Brissaud, F., Seidel, J.-L., Budzinski, H., Elbaz-Poulichet, F., 2006. Consequences of treated water recycling as regards pharmaceuticals and drugs in surface and ground waters of a medium-sized Mediterranean catchment. Environ. Sci. Technol. 40, 5282–5288. https://doi.org/10.1021/es060528p.
Rajamehala, M., Su, R., Gopalakrishnan, B., 2022. Green synthesis of titanium dioxide and its application on anti-fungal activity. Res. J. Pharm. Technol. 15, 695–700.
Rajamohan, N., Rajasimman, M., Dilipkumar, M., 2014. Parametric and kinetic studies on biosorption of mercury using modified *Phoenix dactylifera* biomass. J. Taiwan Inst. Chem. Eng. 45 (5), 2622–2627.
Sahmoune, M.N., 2019. Evaluation of thermodynamic parameters for adsorption of heavy metals by green adsorbents. Environ. Chem. Lett. 17, 697–704. https://doi.org/10.1007/s10311-018-00819-z.
Sarojini, G., Venkateshbabu, S., Rajasimman, M., 2021. Facile synthesis and characterization of polypyrrole - iron oxide – seaweed (PPy-Fe3O4-SW) nanocomposite and its exploration for adsorptive removal of Pb(II) from heavy metal bearing water. Chemosphere 278, 130400. https://doi.org/10.1016/j.chemosphere.2021.130400.
Shaker Ardakani, L., Alimardani, V., Tamaddon, A.M., Amani, A.M., Taghizadeh, S., 2021. Green synthesis of iron-based nanoparticles using Chlorophytum comosum leaf extract: methyl orange dye degradation and antimicrobial properties. Heliyon 7, e06159. https://doi.org/10.1016/j.heliyon.2021.e06159.
Tayyab, M., Liu, Y., Min, S., Muhammad Irfan, R., Zhu, Q., Zhou, L., Lei, J., Zhang, J., 2022. Simultaneous hydrogen production with the selective oxidation of benzyl alcohol to benzaldehyde by a noble-metal-free photocatalyst VC/CdS nanowires. Chin. J. Catal. 43, 1165–1175. https://doi.org/10.1016/S1872-2067(21)63997-9.
Temkin, M.J., Pyzhev, V., 1940. Kinetics of ammonia synthesis on promoted iron catalysts. Acta Phy. Chem. URSS 12, 217–222.
Vasudevan, S., Lakshmi, J., Sozhan, G., 2010. Studies relating to removal of arsenate by electrochemical coagulation: optimization, kinetics, coagulant characterization. Separ. Sci. Technol. 45, 1313–1325. https://doi.org/10.1080/01496391003775949.
Weber, W., Morris, J., 1963. Kinetics of adsorption on carbon from solution. J. Sanit. Eng. Div. 89, 31–59.
Wong, S., Lim, Y., Ngadi, N., Mat, R., Hassan, O., Inuwa, I.M., Mohamed, N.B., Low, J.H., 2018. Removal of acetaminophen by activated carbon synthesized from spent tea leaves: equilibrium, kinetics and thermodynamics studies. Powder Technol. 338, 878–886. https://doi.org/10.1016/j.powtec.2018.07.075.
Yang, Y., Ok, Y.S., Kim, K.-H., Kwon, E.E., Tsang, Y.F., 2017. Occurrences and removal of pharmaceuticals and personal care products (PPCPs) in drinking water and water/sewage treatment plants: a review. Sci. Total Environ. 596, 303–320. https://doi.org/10.1016/j.scitotenv.2017.04.102. –597.
Yuh-Shan, H., 2004. Citation review of Lagergren kinetic rate equation on adsorption reactions. Scientometrics 59, 171–177. https://doi.org/10.1023/B:SCIE.0000013305.99473.cf.
Żur, J., Wojcieszyńska, D., Hupert-Kocurek, K., Marchlewicz, A., Guzik, U., 2018. Paracetamol - toxicity and microbial utilization. Pseudomonas moorei KB4 as a case study for exploring degradation pathway. Chemosphere 206, 192–202. https://doi.org/10.1016/j.chemosphere.2018.04.179.